

# Two-impurity helical Majorana problem

Erik Eriksson,<sup>1</sup> Alex Zazunov,<sup>1</sup> Pasquale Sodano,<sup>2,3,4</sup> and Reinhold Egger<sup>1,2</sup>

<sup>1</sup>*Institut für Theoretische Physik, Heinrich-Heine-Universität, D-40225 Düsseldorf, Germany*

<sup>2</sup>*International Institute of Physics, Universidade Federal do Rio Grande do Norte, 59078-400 Natal-RN, Brazil*

<sup>3</sup>*Departamento de Física Teórica e Experimental,*

*Universidade Federal do Rio Grande do Norte, 59072-970 Natal-RN, Brazil*

<sup>4</sup>*INFN, Sezione di Perugia, Via A. Pascoli, 06123 Perugia, Italy*

(Dated: February 13, 2015)

We predict experimentally accessible signatures for helical Majorana fermions in a topological superconductor by coupling to two quantum dots in the local moment regime (corresponding to spin-1/2 impurities). Taking into account RKKY interactions mediated by bulk and edge modes, where the latter cause a long-range antiferromagnetic Ising coupling, we formulate and solve the low-energy theory for this two-impurity helical Majorana problem. In particular, we show that the long-time spin dynamics after a magnetic field quench displays weakly damped oscillations with universal quality factor.

PACS numbers: 74.78.-w, 73.21.-b, 74.40.-n

## I. INTRODUCTION

Over the past few years, several groups have reported first experimental signatures for the elusive Majorana bound state in superconducting hybrid devices [1–5]. Majorana bound states exist near the ends of topologically nontrivial one-dimensional (1D) superconductors, and many proposals have appeared on how to probe them [6–16]. Likewise, the boundary of a 2D topological superconductor (TS) can host propagating gapless Majorana fermion states [6, 17], with different properties as compared to the mostly studied Majorana bound states. Recent experiments on InAs/GaSb [18, 19], HgTe/CdTe [20], or topological insulator [21] heterostructures with  $s$ -wave superconductors have indeed reported an edge-state dominated Fraunhofer pattern of the Josephson current.

These developments highlight the urgent need for realistic proposals on how to prepare, manipulate, and detect 1D Majorana edge states. We here consider the case of a time-reversal symmetric 2D TS with counterpropagating (right- and left-moving) Majorana edge states of opposite spin polarization [6, 17]. A major obstacle to the detection of these “helical” Majorana modes arises from their charge neutrality. As a consequence, transport experiments are difficult, requiring one to study thermal transport or interferometric devices [22–26]. Moreover, although a zero-bias tunneling conductance peak due to the Majorana edge is expected [11], similar peaks are also caused by other mechanisms [8].

We here propose a setup, see Fig. 1, where the physics of helical Majorana fermions can be probed in a direct and realistic manner through their coupling to two quantum dots located near the boundary of a 2D TS, see Fig. 1. Assuming a standard parameter regime with strongly repulsive on-dot Coulomb interaction, each dot corresponds to a spin-1/2 operator [27]. We imagine that the dots are arranged slightly above the superconducting plane, with an insulating layer separating them from the TS. Tunnel couplings connecting the dots to the Majorana edge then imply the presence of an exchange coupling,  $J$ , to the Ising spin density of the Majorana edge at the respective location. (In what follows, we often refer to the dots simply as “spins.”) The corresponding single-dot case was studied in Ref. [28], and Kondo physics was found in a magnetic field. However, the predicted quantum phase transition occurs only for unphysical parameter values [29].

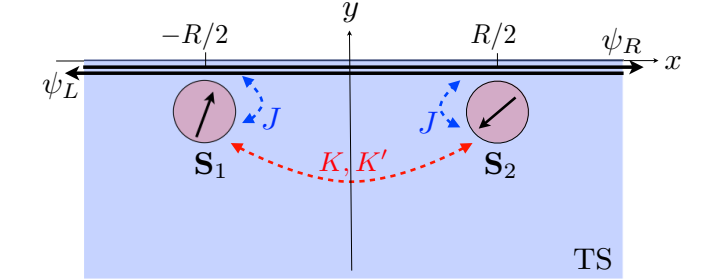


Figure 1. Schematic setup: Two quantum dots located near the helical Majorana edge states of a 2D TS which occupies the  $xy$  half-plane with  $y < 0$ . For strong on-site repulsion, the dots are equivalent to spin-1/2 operators,  $\mathbf{S}_1$  and  $\mathbf{S}_2$ , respectively, separated by a distance  $R$ . They are exchange-coupled ( $J$ ) to the local Ising spin density of the Majorana edge, and RKKY-coupled to each other ( $K, K'$ ) through bulk TS modes.

For two dots, see Fig. 1, we instead encounter a Majorana version of the classic two-impurity Kondo problem [30]. In this setup, we predict clear signatures of the helical Majorana edge to appear in the “spin” dynamics of the dots. The rich physics found for the two-impurity helical Majorana problem arises from the interplay between Ising-like exchange couplings and indirect Ruderman-Kittel-Kasuya-Yosida (RKKY) spin-spin interactions [31] mediated by the TS. We find that the Majorana edge causes long-range RKKY contributions, which we nonperturbatively determine below. In addition,

tion, bulk TS modes mediate an SU(2)-symmetric ferromagnetic RKKY coupling ( $K$ ), plus an Ising-type antiferromagnetic coupling ( $K'$ ) [32]. These couplings are especially pronounced when the spins bind Shiba states inside the TS gap [33].

Before turning to derivations and detailed discussions, let us briefly summarize our main results. (i) The low-energy theory for the two-impurity helical Majorana problem can be solved analytically. In the zero-field case, for a wide parameter regime, we find that the ground state is a fully entangled triplet state of both spins even when they are widely separated. This long-range entanglement is rather unique and of interest in quantum information applications [34]. (ii) The helical Majorana edge causes an Ising-type antiferromagnetic RKKY coupling,  $K_M \sim J^2/R$ , which exhibits a slow decay with spin-spin distance  $R$ . This result holds for arbitrary  $J$ , even though conventional RKKY theory assumes small  $J$ . (iii) Experimentally monitoring the weakly damped spin dynamics after a magnetic field quench allows one to extract clear signatures for helical Majorana fermions through the predicted universal quality factor, see Eq. (39) below. The magnetic fields can be produced by using ferromagnetic finger gates. Time-dependent measurements of the dot spins can be performed with high precision using available state tomography techniques, see, e.g., Refs. [35–37]. The setup in Fig. 1 thus offers a direct way to manipulate and detect the helical Majorana fermion edge state of a 2D time-reversal invariant TS. Apart from the above-mentioned platforms, our predictions also apply to bilayer Rashba quantum wells [38] and exotic triplet-paired superconductors [6–8].

The structure of the remainder of this paper is as follows. In Sec. II, we introduce the setup and the theoretical model to describe it. We then turn to the perturbative regime of small  $J$  in Sec. III, where we derive the RKKY interaction mediated by the Majorana edge. In addition, we provide an explicit solution of the problem at not too low energy scales. The low-energy regime is then discussed in Sec. IV, where we show that the problem can be mapped to a dissipative quantum impurity problem. Concrete predictions for the resulting spin-boson like dynamics are presented in Sec. V, where we also comment on the unique signatures of helical Majorana fermions in such experiments. Finally, we conclude with a brief summary in Sec. VI. Throughout the paper, we work in units with  $\hbar = k_B = 1$ .

## II. MODEL

We consider a time-reversal symmetric 2D TS located in the  $xy$  half-plane  $y < 0$ , which hosts 1D helical Majorana fermions near the edge. On energy scales below the bulk TS gap  $\Delta$ , the TS Hamiltonian reduces to the gapless edge contribution [17]

$$H_0 = -iv \int_{-\infty}^{\infty} dx (\psi_R \partial_x \psi_R - \psi_L \partial_x \psi_L), \quad (1)$$

with self-adjoint Majorana field operators,  $\psi_\nu(x) = \psi_\nu^\dagger(x)$ , subject to the anticommutator algebra

$$\{\psi_\nu(x), \psi_{\nu'}(x')\} = \delta_{\nu\nu'} \delta(x - x'), \quad (2)$$

where  $\nu = R, L$ . Weak time-reversal invariant perturbations, e.g., due to spin-orbit coupling or elastic disorder, cannot gap out the edge state and may only renormalize the edge velocity  $v$ .

Importantly, because of the Majorana anticommutator algebra, the spin density operator has only one nonvanishing component,

$$s(x) = i\psi_R(x)\psi_L(x). \quad (3)$$

This Ising property reflects the Majorana “half-fermion” character and is in contrast to helical Dirac fermions, where only expectation values of the other spin density components vanish but not the operators themselves. The corresponding “Ising direction”,  $\hat{e}_I$ , of the spin polarization depends on the actual TS realization [6]. In most applications, the Ising direction is in the TS plane. We therefore put

$$\hat{e}_I = (\cos \theta, \sin \theta, 0). \quad (4)$$

For instance, using the same coordinates as in Fig. 1, we find  $\theta = 0$  for the TS realizations in Refs. [28, 32], while  $\theta = \pi/2$  for the Fu-Kane proposal [17].

Next we consider two quantum dots at  $x = \mp R/2$  near the edge of the TS. In experimental realizations, the dots could be displaced away from the TS plane along the  $z$ -axis, with finite tunnel couplings to both the Majorana edge and to bulk TS modes, see Fig. 1. Taking dot parameters within the standard local-moment regime of strong on-site Coulomb interaction [27], the dots correspond to spin-1/2 operators  $\mathbf{S}_1$  and  $\mathbf{S}_2$ , respectively. With  $s(x)$  in Eq. (3), tunnel couplings between the dots and the Majorana edge imply Ising exchange couplings [29],

$$H_J = J [s(-R/2)S_{I,1} + s(R/2)S_{I,2}], \quad (5)$$

where we assume the same  $J$  for both spins, and  $S_{I,j=1,2}$  denotes the projection of the respective spin operator to the Ising direction,

$$S_{I,j} = \hat{e}_I \cdot \mathbf{S}_j = S_{x,j} \cos \theta + S_{y,j} \sin \theta. \quad (6)$$

Although gapped bulk TS modes do not appear in Eq. (1), they are important in mediating RKKY interactions between  $\mathbf{S}_1$  and  $\mathbf{S}_2$ . Treating the exchange coupling,  $J_b$ , between the spins and the bulk TS modes perturbatively, see Ref. [32], the full Hamiltonian reads

$$H = H_0 + H_J + H_D, \quad (7)$$

with

$$H_D = -K \mathbf{S}_1 \cdot \mathbf{S}_2 + K' S_{y,1} S_{y,2} - \mathbf{B} \cdot (\mathbf{S}_1 + \mathbf{S}_2). \quad (8)$$

Note that  $H_D$  does not include the edge-mediated RKKY interaction. For  $R \ll \xi = v_b/\Delta$ , where  $\xi$  is the superconducting coherence length and  $v_b$  the bulk Fermi velocity, the bulk-induced RKKY couplings are estimated as

$$K \approx \frac{J_b^2}{16\pi v_b R^3}, \quad K' \approx \frac{3K}{2}. \quad (9)$$

For the case of arbitrary  $R/\xi$ , see Ref. [32]. The SU(2)-invariant term  $\sim K$  in Eq. (8) favors ferromagnetic alignment of both spins, while the Ising term  $\sim K'$  favors antiferromagnetic alignment along the  $y$ -axis.

We note that similar RKKY interactions also appear in the conventional two-impurity Kondo problem once spin-orbit couplings are taken into account [39, 40]. However, here we have  $k_F = 0$  because of particle-hole symmetry, and the usual  $2k_F$ -oscillations with distance, see Ref. [31], are completely absent in our case.

Finally, we have also included a magnetic Zeeman field proportional to  $\mathbf{B} = (B_x, B_y, B_z)$  in Eq. (8), which is assumed to act only on the total dot spin. Such a field could be produced by suitable ferromagnetic finger gates. Without loss of generality, we put  $B_y \geq 0$ .

The model (7) describes the two-impurity helical Majorana problem. It differs from the two-impurity Kondo problem for Dirac fermions [30], which hosts Kondo physics and an unstable non-Fermi liquid fixed point. This difference is present even when allowing for spin-orbit induced anisotropy effects in the conventional problem [39, 40], and can be rationalized by noting that for the Majorana case, we have exchange couplings connecting the impurity spins to the Ising spin density only. As we show in detail below, this distinction leads to rather different physics as compared to the results in Refs. [30, 39, 40].

### III. MAJORANA-MEDIATED RKKY INTERACTION AND PERTURBATIVE SOLUTION

We begin our analysis with the small- $J$  limit. The effect of the Majorana edge on the spin dynamics can then be taken into account by perturbation theory in  $J$ . After some algebra, we obtain the additional Ising-like RKKY contribution,

$$H_M = K_M S_{I,1} S_{I,2}, \quad K_M = \frac{\pi v}{4R} (\rho_0 J)^2, \quad (10)$$

with the density of states  $\rho_0 = 1/(2\pi v)$  of the Majorana edge. In contrast to the bulk-induced Ising-like RKKY term  $\sim K'$  in Eq. (8), the anisotropy axis is now set by  $\hat{e}_I$ . Note that the slow  $1/R$  decay of  $K_M$  is as for conventional 1D Dirac fermions. In fact, by replacing  $\rho_0 \rightarrow 2\rho_0$  in Eq. (10), the  $k_F = 0$  Ising variant of the well-known 1D RKKY coupling [41, 42] is recovered.

For small  $J$ , the coupled spin dynamics is thus captured by the effective Hamiltonian

$$H_{\text{eff}} = H_D + H_M. \quad (11)$$

With the total spin operator,

$$\mathbf{S} = \mathbf{S}_1 + \mathbf{S}_2, \quad (12)$$

we then obtain

$$H_{\text{eff}} = -\frac{K}{2} \mathbf{S}^2 + \frac{K_M \cos^2 \theta}{2} S_x^2 + \frac{K' + K_M \sin^2 \theta}{2} S_y^2 - \mathbf{B} \cdot \mathbf{S}. \quad (13)$$

Using singlet ( $S = M = 0$ ) and triplet ( $S = 1$  with  $M = 0, \pm 1$ ) states with spin quantization axis along the  $y$ -direction,

$$\mathbf{S}^2 |S, M\rangle = S(S+1) |S, M\rangle, \quad S_y |S, M\rangle = M |S, M\rangle, \quad (14)$$

the singlet state decouples and the remaining  $3 \times 3$  matrix representation for  $H_{\text{eff}}$  can be readily diagonalized.

To illustrate the physics described by Eq. (13), we now consider the case  $B_x = B_z = 0$ . To simplify expressions, it is convenient to shift the overall energy scale such that the singlet state  $|0, 0\rangle$ , which is always an eigenstate, has the energy  $E_s = K$ . The triplet state  $|1, 0\rangle$ , with  $M = 0$ , is also an eigenstate with energy

$$E_{t,0} = (K_M/2) \cos^2 \theta. \quad (15)$$

The  $M = -1$  and  $M = +1$  triplet states hybridize, resulting in the energies

$$E_{t,\pm} = \frac{2K' + K_M(1 + \sin^2 \theta)}{4} \pm \sqrt{B_y^2 + (K_M/4)^2 \cos^4 \theta}. \quad (16)$$

We now discuss the resulting ground state for  $\mathbf{B} = 0$  with  $\theta = \pi/2$  and  $\theta = 0$ , respectively.

First, when the Ising direction is oriented along the  $y$ -axis, i.e., for  $\theta = \pi/2$ , noting that all RKKY couplings ( $K, K', K_M$ ) are positive, we find that the entangled triplet state  $|1, 0\rangle$  is always the ground state. This state minimizes both the ferromagnetic SU(2)-symmetric RKKY term  $\sim K$  and the antiferromagnetic Ising RKKY interaction  $\sim K' + K_M$ . For typical parameters [32] and  $R \approx 10$  nm, the excitation energies above this ground state correspond to temperatures  $\approx 1 \dots 10$  K. At lower temperatures, both dots are therefore fully entangled due to TS-mediated long-range RKKY interactions.

Second, for  $\theta = 0$ , using  $K' \approx 3K/2$ , we see in a similar fashion that the ground state is either again the triplet state,  $|1, 0\rangle$  for  $R > R_c$ , or it corresponds to  $E_{t,-}$  for  $R < R_c$ . As the spin-spin distance  $R$  is varied through a critical value  $R_c$  determined by  $K'(R_c) = K_M(R_c)$ , we thus observe that a quantum phase transition occurs. This transition is caused by the competition between the Majorana- and the bulk-induced Ising-like RKKY terms, which have different anisotropy axes for  $\theta \neq \pi/2$ .

### IV. LOW-ENERGY THEORY

In this section, we turn to the low-energy regime and thereby discuss the physics beyond the perturbative

small- $J$  regime. To start, let us combine the Majorana fields into a chiral Dirac fermion field, see also Ref. [28],

$$\Psi(x) = \frac{1}{\sqrt{2}} (\psi_R(x) + i\psi_L(-x)), \quad (17)$$

where Eq. (1) yields the equivalent form

$$H_0 = -iv \int dx \Psi^\dagger \partial_x \Psi. \quad (18)$$

The Ising exchange term in Eq. (5) then reads

$$H_J = \frac{1}{2} J S_I [\Psi^\dagger(R/2) \Psi(-R/2) + \text{h.c.}] \\ + \frac{1}{2} J (S_{I,1} - S_{I,2}) [\Psi^\dagger(R/2) \Psi^\dagger(-R/2) + \text{h.c.}] \quad (19)$$

with the total spin

$$S_I = S_{I,1} + S_{I,2}. \quad (20)$$

Note that  $H_J$  effectively describes non-local single-particle processes of either potential scattering or pairing type.

On energy scales below  $v/R$ , however, the non-locality present in Eq. (19) generates only corrections that are irrelevant in the renormalization group (RG) sense. Indeed, we find that the low-energy expansion,  $H_J \rightarrow H_J^{(1)} + H_J^{(2)}$ , comes from the local operators

$$H_J^{(1)} = J S_I \Psi^\dagger(0) \Psi(0), \quad (21) \\ H_J^{(2)} = \frac{J R}{2} (S_{I,1} - S_{I,2}) \Psi^\dagger(0) \partial_x \Psi^\dagger(0) + \text{h.c.}$$

The term  $H_J^{(1)}$  is precisely marginal (scaling dimension 1), while the leading irrelevant operator  $H_J^{(2)}$  has scaling dimension 2. Performing a standard one-loop RG analysis, using the operator product expansions for the fermion operators in Eq. (21), it immediately follows that the only new operator generated during the RG flow is precisely the RKKY term (10). The  $H_J^{(1)}$  term does not renormalize, whereas the  $H_J^{(2)}$  term flows to zero. Hence we conclude that  $H_J^{(2)}$  can safely be taken into account by renormalization of  $K_M$ , and the fermionic low-energy theory is given by

$$H_f = H_0 + H_J^{(1)}. \quad (22)$$

To proceed further, we now bosonize the chiral fermion in Eq. (17), see Ref. [27],

$$\Psi(x) = \frac{1}{\sqrt{2\pi R}} e^{-i\phi(x)}, \quad (23)$$

using the chiral boson field  $\phi(x)$  with commutator

$$[\phi(x), \phi(x')]_- = i\pi \text{sgn}(x - x'), \quad (24)$$

where  $R$  is taken as short-distance cutoff length. The Euclidean action corresponding to  $H_f$  is then given by

$$S_f = -\frac{1}{4\pi} \int dx d\tau \partial_x \phi (i\partial_\tau + v\partial_x) \phi \\ + v\rho_0 J \int d\tau S_I(\tau) \partial_x \phi(0, \tau), \quad (25)$$

where  $S_I(\tau)$  is a discrete imaginary-time spin path. The benefit of this step is that we have a Gaussian action for the bosonic field variables, which can therefore be integrated out exactly.

Performing the Gaussian field integration over  $\phi$ , we finally obtain the effective spin action

$$S_{\text{spin}} = -\frac{1}{2} (\rho_0 J)^2 \int d\tau d\tau' \frac{S_I(\tau) S_I(\tau')}{(\tau - \tau')^2 + (R/v)^2} \\ + (v/R) (\rho_0 J)^2 \int d\tau S_I^2(\tau). \quad (26)$$

The first term corresponds to Ohmic damping [28, 43, 44]. We mention in passing that this term vanishes for a constant spin path,  $S_I(\tau) = 0, \pm 1$ . The second term instead describes once again the RKKY coupling  $K_M$  due to the Majorana edge. As expected from the chiral anomaly of 1D fermions [27], no orders higher than  $J^2$  appear in Eq. (26). This indicates that up to a prefactor of order unity, Eq. (10) stays in fact valid beyond the perturbative small- $J$  regime.

We now show that, up to an overall irrelevant energy shift, the low-energy Hamiltonian for the two spins can be written as

$$H = H_{\text{eff}} + (S_x \cos \theta + S_y \sin \theta) \mathcal{E} + H_B[\mathcal{E}], \quad (27)$$

where  $\mathcal{E}$  is a Gaussian random field with zero mean and  $H_{\text{eff}}$  is defined in Eq. (13). The “bath” Hamiltonian  $H_B$  here describes an infinite set of harmonic oscillators generating the correlation function

$$L(z) = \langle \mathcal{E}(0) \mathcal{E}(z) \rangle_B \quad (28)$$

for complex time  $z = t - i\tau$ . To show the correctness of Eq. (27), we note that when averaging the partition function corresponding to Eq. (27) over the Gaussian random field  $\mathcal{E}$ , we should arrive back at the effective two-impurity action (26) [43]. This procedure allows us to determine the bath correlation function  $L(z)$ . Indeed, by averaging over  $\mathcal{E}$  and comparison to Eq. (26), we find that Eq. (28) must be given by

$$L(z) = \frac{1}{\pi} \int_0^\infty d\omega J(\omega) \frac{\cosh[\omega(-iz + \beta/2)]}{\sinh[\beta\omega/2]}. \quad (29)$$

In Eq. (29), we allow for finite temperature  $T = 1/\beta$  and state the result for complex time  $z = t - i\tau$ . The correlation function  $L(z)$  is here expressed in terms of a so-called Ohmic spectral density [43],

$$J(\omega) = 2\pi\alpha\omega e^{-\omega/(v/R)}, \quad (30)$$

which in turn contains the dimensionless damping parameter

$$\alpha = \frac{1}{2}(\rho_0 J)^2. \quad (31)$$

For physically relevant parameters, the damping strength is small,  $\alpha \ll 1$ . For  $T = 0$ , Eq. (29) then yields a characteristic inverse-square time dependence,

$$L_{T=0}(z) = -\frac{2\alpha}{(z - iR/v)^2}. \quad (32)$$

The general formulation in Eq. (27) offers a convenient starting point to discuss the dissipative real-time dynamics of the two coupled spins.

## V. DISSIPATIVE TWO-IMPURITY SPIN DYNAMICS

In what follows, we consider this effective spin dynamics in a magnetic field and show that it contains unique signatures of the underlying helical Majorana fermions. For clarity, we here choose the Ising direction corresponding to  $\theta = \pi/2$  and put  $B_z = 0$ , but we believe that our conclusions apply generally.

Using the parameter

$$\epsilon = -B_y + (K' + K_M)/2, \quad (33)$$

we first observe from Eq. (16) that for  $B_x = 0$ , the field component  $B_y$  along the Ising direction drives a quantum phase transition from the entangled  $|1, 0\rangle$  state, which is the ground state for  $\epsilon > 0$ , to the separable polarized triplet state  $|1, 1\rangle$  for  $\epsilon < 0$ . In fact, assuming that the system parameters are in the regime

$$\max\{|\epsilon|, |B_{x,z}|, T\} \ll K, \quad (34)$$

it is justified to project Eq. (27) to the subspace spanned by  $|1, 1\rangle$  and  $|1, 0\rangle$  only. Defining Pauli matrices  $\sigma_{x,z}$  in that subspace, such a projection arrives at the well-known spin-boson model [45],

$$H_{\text{SB}} = -\frac{B_x}{\sqrt{2}}\sigma_x + \frac{\epsilon + \mathcal{E}}{2}\sigma_z + H_B. \quad (35)$$

Since the damping parameter  $\alpha$  in Eq. (31) is small, the spin dynamics found after a sudden change (“quench”) of the magnetic field will then show weakly damped oscillations. For instance, taking a constant field component  $B_x$  and suddenly switching  $B_y$  at time  $t = 0$ , such that we have a large negative  $\epsilon$  at  $t < 0$  but a vanishing value afterwards,  $\epsilon(t > 0) = 0$ , the  $T = 0$  spin dynamics follows from the exact long-time result [46]

$$\langle \sigma_z(t) \rangle \sim e^{-\Gamma t} \cos(\Omega t), \quad (36)$$

where the average is taken using  $H_{\text{SB}}$ . The physical spin dynamics then follows from the relation

$$\langle S_y(t) \rangle = \frac{1}{2} (\langle \sigma_z(t) \rangle + 1). \quad (37)$$

Equation (36) is characterized by the damping rate

$$\Gamma = 2T_b \sin^2 \left( \frac{\pi\alpha}{2(1-\alpha)} \right), \quad (38)$$

and by the quality factor  $Q$  connecting the damping rate to the oscillation frequency,

$$Q = \frac{\Omega}{\Gamma} = \cot \left( \frac{\pi\alpha}{2(1-\alpha)} \right). \quad (39)$$

Importantly, the quality factor is universal in the sense that it is independent of  $B_x$  or other microscopic parameters. In Eq. (38), we use the energy scale

$$T_b = c_b (RB_x/v)^{\alpha/(1-\alpha)} B_x, \quad (40)$$

where  $c_b$  is a prefactor of order unity (for its precise value, see Ref. [43]). The above reasoning suggests that an experimental observation of damped spin oscillations with universal ( $B_x$ -independent) quality factor, see Eq. (39), constitutes a nontrivial signature for helical Majorana fermions.

## VI. CONCLUSIONS

In this work, we have proposed to couple two quantum dots in the local moment regime (where they correspond to spin-1/2 impurities) to the helical Majorana edge states of a 2D topological superconductor. The superconductor then causes edge- and bulk-induced RKKY interactions among the two spins, where the resulting low-energy theory can be solved in an essentially exact manner. Notably, the physics found for this two-impurity helical Majorana problem strongly differs from the respective helical Dirac problem, see also Ref. [47]. In the presence of time-dependent magnetic fields, the spin dynamics is characterized by weakly damped coherent oscillations with universal quality factor. In a setup as shown in Fig. 1, we believe that such oscillations could be reliably measured by available state tomography techniques [35–37].

## ACKNOWLEDGMENTS

We thank A. Tavanfar for useful discussions. R.E. acknowledges support by SPP 1666 of Deutsche Forschungsgemeinschaft and by CNPq program Science Without Borders (SWB). P.S. thanks the Ministry of Science, Technology, and Innovation of Brazil and CNPq for granting a “Bolsa de Produtividade em Pesquisa”, and acknowledges support by the CNPq SWB program, and from MCTI and UFRN/MEC (Brazil).

- 
- [1] V. Mourik, K. Zuo, S.M. Frolov, S.R. Plissard, E.P.A.M. Bakkers, and L.P. Kouwenhoven, *Science* **336**, 1003 (2012).
- [2] L. Rokhinson, X. Liu, and J. Furdyna, *Nat. Phys.* **8**, 795 (2012).
- [3] A. Das, Y. Ronen, Y. Most, Y. Oreg, M. Heiblum, and H. Shtrikman, *Nat. Phys.* **8**, 887 (2012).
- [4] M.T. Deng, C.L. Yu, G.Y. Huang, M. Larsson, P. Caroff, and H.Q. Xu, *Nano Lett.* **12**, 6414 (2012).
- [5] S. Nadj-Perge, I.K. Drozdov, J. Li, H. Chen, S. Jeon, J. Seo, A.H. MacDonald, B.A. Bernevig, and A. Yazdani, *Science* **446**, 602 (2014).
- [6] X.L. Qi and S.C. Zhang, *Rev. Mod. Phys.* **83**, 1057 (2011).
- [7] Y. Tanaka, M. Sato, and N. Nagaosa, *J. Phys. Soc. Jpn.* **81**, 011013 (2012).
- [8] J. Alicea, *Rep. Prog. Phys.* **75**, 075061 (2012).
- [9] M. Leijnse and K. Flensberg, *Semicond. Sci. Technol.* **27**, 124003 (2012).
- [10] C.W.J. Beenakker, *Annu. Rev. Condens. Matter Phys.* **4**, 113 (2013).
- [11] K.T. Law, P.A. Lee, and T.K. Ng, *Phys. Rev. Lett.* **103**, 237001 (2009).
- [12] E. Eriksson, C. Mora, A. Zazunov, and R. Egger, *Phys. Rev. Lett.* **113**, 076404 (2014).
- [13] D.E. Liu and H.U. Baranger, *Phys. Rev. B* **84**, 201308(R) (2011).
- [14] J.D. Sau and S. Das Sarma, *Nature Comm.* **3**, 964 (2012).
- [15] M. Leijnse and K. Flensberg, *Phys. Rev. B* **86**, 134528 (2012).
- [16] E. Vernek, P.H. Penteado, A.C. Seridonio, and J.C. Egues, *Phys. Rev. B* **89**, 165314 (2014).
- [17] L. Fu and C.L. Kane, *Phys. Rev. Lett.* **100**, 096407 (2008).
- [18] I. Knez, R.R. Du, and G. Sullivan, *Phys. Rev. Lett.* **109**, 186603 (2012).
- [19] V.S. Pribiag, A.J.A. Beukman, F. Qu, M.C. Cassidy, C. Charpentier, W. Wegscheider, and L.P. Kouwenhoven, *arXiv:1408.1701*.
- [20] S. Hart, H. Ren, T. Wagner, P. Leubner, M. Mühlbauer, C. Brüne, H. Buhmann, L.W. Molenkamp, and A. Yacoby, *Nat. Phys.* **10**, 638 (2014).
- [21] S.Y. Xu *et al.*, *Nat. Phys.* **10**, 943 (2014).
- [22] Y. Asano, Y. Tanaka, and N. Nagaosa, *Phys. Rev. Lett.* **105**, 056402 (2010).
- [23] C.X. Liu and B. Trauzettel, *Phys. Rev. B* **83**, 220510(R) (2011).
- [24] B. Béri, *Phys. Rev. B* **85**, 140501(R) (2012).
- [25] M. Diez, I.C. Fulga, D.I. Pikulin, M. Wimmer, A.R. Akhmerov, and C.W.J. Beenakker, *Phys. Rev. B* **87**, 125406 (2013).
- [26] B.J. Wieder, F. Zhang, and C.L. Kane, *Phys. Rev. B* **89**, 075106 (2014).
- [27] A. Altland and B.D. Simons, *Condensed Matter Field Theory* (Cambridge University Press, Cambridge, UK, 2010).
- [28] R. Shindou, A. Furusaki, and N. Nagaosa, *Phys. Rev. B* **82**, 180505(R) (2010).
- [29] R. Zitko and P. Simon, *Phys. Rev. B* **84**, 195310 (2011).
- [30] B.A. Jones and C.M. Varma, *Phys. Rev. Lett.* **58**, 843 (1987); B.A. Jones, C.M. Varma, and J.W. Wilkins, *Phys. Rev. Lett.* **61**, 125 (1988); J. Gan, *Phys. Rev. B* **51**, 8287 (1995); I. Affleck, A.W.W. Ludwig, and B.A. Jones, *Phys. Rev. B* **52**, 9528 (1995).
- [31] M.A. Ruderman and C. Kittel, *Phys. Rev.* **96**, 99 (1954); T. Kasuya, *Prog. Theor. Phys.* **16**, 45 (1956); K. Yosida, *Phys. Rev.* **106**, 893 (1957).
- [32] A.A. Zyuzin and D. Loss, *Phys. Rev. B* **90**, 125443 (2014).
- [33] N.Y. Yao, L.I. Glazman, E.A. Demler, M.D. Lukin, and J.D. Sau, *Phys. Rev. Lett.* **113**, 087202 (2014).
- [34] R. Horodecki, P. Horodecki, M. Horodecki, and K. Horodecki, *Rev. Mod. Phys.* **81**, 865 (2009).
- [35] R. Hanson, L.P. Kouwenhoven, J.R. Petta, S. Tarucha, and L.M.K. Vandersnypen, *Rev. Mod. Phys.* **79**, 1217 (2007).
- [36] J. Medford *et al.*, *Nat. Nanotech.* **8**, 654 (2013).
- [37] P. Roushan *et al.*, *Nature* **515**, 241 (2014).
- [38] S. Nakosai, Y. Tanaka, and N. Nagaosa, *Phys. Rev. Lett.* **108**, 147003 (2012).
- [39] D.F. Mross and H. Johannesson, *Phys. Rev. B* **80**, 155302 (2009).
- [40] M. Garst, S. Kehrein, T. Pruschke, A. Rosch, and M. Vojta, *Phys. Rev. B* **69**, 214413 (2004).
- [41] Y. Yafet, *Phys. Rev. B* **36**, 3948 (1987).
- [42] V.I. Litvinov and V.K. Dugaev, *Phys. Rev. B* **58**, 3584 (1998).
- [43] U. Weiss, *Quantum Dissipative Systems*, 4th ed. (World Scientific, Singapore, 2012).
- [44] Bulk TS modes are gapped and produce no low-frequency contributions to damping.
- [45] A.J. Leggett, S. Chakravarty, A.T. Dorsey, M.P.A. Fisher, A. Garg, and W. Zwerger, *Rev. Mod. Phys.* **59**, 1 (1986).
- [46] F. Lesage and H. Saleur, *Phys. Rev. Lett.* **80**, 4370 (1998).
- [47] J. Maciejko, *Phys. Rev. B* **85**, 245108 (2012).